Supporting Information

All small molecule organic solar cells based on an electron donor incorporating binary electron-deficient units

Guitao Feng,[a,b] Yunhua Xu,*[a] Jianqi Zhang,[c] Zhaowei Wang,[d] Yi Zhou,[d] Zhixiang Wei,[c] Yongfang Li,[d] Cheng Li*[b] and Weiwei Li*[b]

[a] *Department of Chemistry, School of Science, Beijing Jiaotong University, Beijing 100044, China. yhxu@bjtu.edu.cn.*

[b] *Beijing National Laboratory for Molecular Sciences, CAS Key Laboratory of Organic Solids, Institute of Chemistry, Chinese Academy of Sciences, Beijing 100190, P. R. China. E-mail: licheng1987@iccas.ac.cn, liweiwei@iccas.ac.cn*

[c] *National Center for Nanoscience and Technology, Chinese Academy of Sciences, Beijing 100190, China.*

[d] *Laboratory of Advanced Optoelectronic Materials, College of Chemistry, Chemical Engineering and Materials Science, Soochow University, Suzhou, Jiangsu 215123, China*

Contents

1. Absorption spectra of PCLDPP in solution and thin films

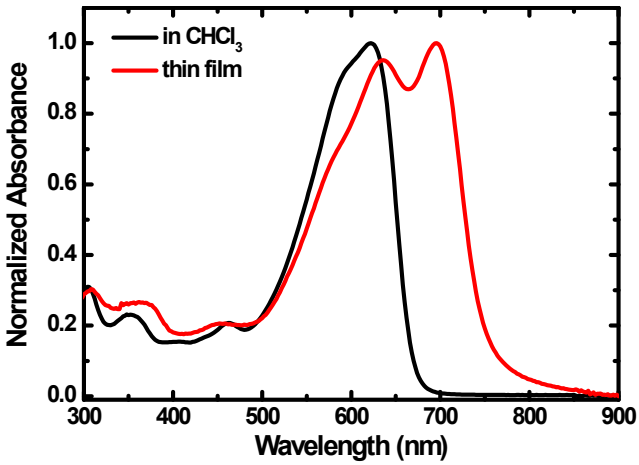

Fig. S1 Absorption spectra of the molecular PCLDPP in $CHCl_3$ solution and solid state films. The absorption onset of PCLDPP in $CHCl_3$ solution is 675 nm with E_g^{CHCl3} = 1.84 eV.

2. Cyclic voltammetry

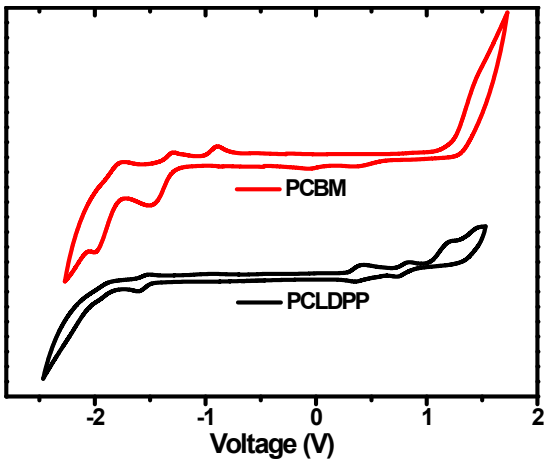

Fig. S2 Cyclic voltammogram of the molecular PCLDPP and PCBM in CH_2Cl_2. Potential vs. Fc/Fc^+.

3. DFT calculations

Density function theory (DFT) calculations were performed at the B3LYP/6-31G* level of theory by using the Gaussian 09 program package.

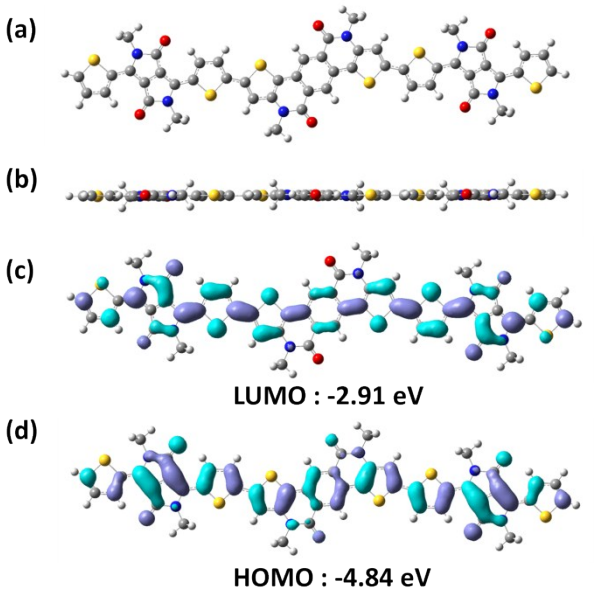

Fig. S3 DFT calculations of the DPP-PCL-DPP segment. (a) Front view and (b) side view of the optimized molecular geometry. (c) and (d) Frontier molecular orbitals.

4. AFM of PCLDPP thin films

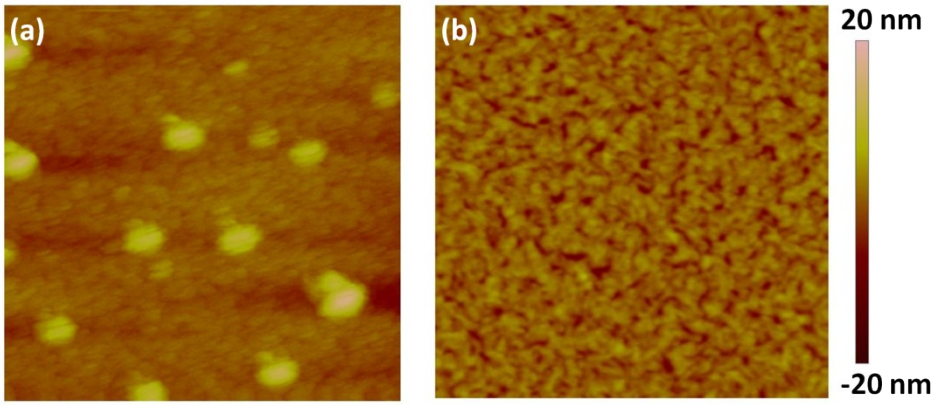

Fig. S4 AFM height image of PCLDPP thin films on Si substrate (a) without and (b) with thermal annealing at 80 °C. The root mean square (RMS) roughness values of (a) and (b) are 1.00 nm and 2.02 nm.

5. Solar cells of PCLDPP:PCBM

Table S1. Characteristics of PCLDPP:PCBM (1:1) solar cells fabricated from chloroform without or with different content of DIO as additive.

Solvent	Thickness	J_{sc}[a]	V_{oc}	FF	PCE[a]

	(nm)	(mA/cm^2)	(V)		(%)
$CHCl_3$	100	3.7	0.84	0.55	1.7
$CHCl_3$:0.2% DIO	100	5.6	0.86	0.56	2.7
$CHCl_3$:0.5% DIO	95	9.7	0.89	0.56	4.8
$CHCl_3$:1% DIO	90	8	0.89	0.50	3.6
$CHCl_3$:2.5% DIO	100	9.9	0.88	0.51	4.5
$CHCl_3$:4% DIO	100	8.2	0.86	0.49	3.5

[a] J_{sc} as calculated by integrating the EQE spectrum with the AM1.5 G spectrum.

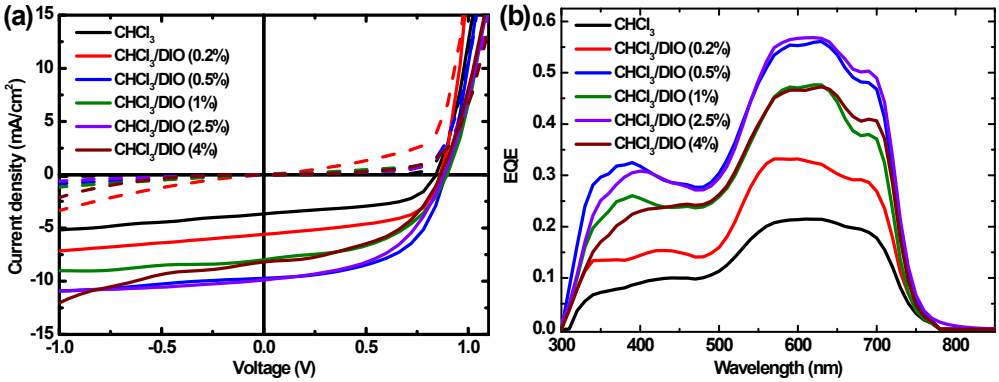

Fig. S5 (a) *J-V* characteristics under white light illumination and (b) EQE of the PCLDPP:PCBM (1:1) solar cells fabricated from $CHCl_3$ without or with different content of DIO as additive.

Table S2. Characteristics of PCLDPP:PCBM solar cells fabricated from $CHCl_3$/DIO (2%) with different ratio of donor to acceptor.

Ratio	Thickness (nm)	J_{sc}[a] (mA/cm^2)	V_{oc} (V)	FF	PCE[a] (%)
2:1	120	9.6	0.88	0.50	4.2
1:1	95	9.7	0.89	0.56	4.8
1:2	110	7.8	0.88	0.54	3.7
1:3	100	6.4	0.87	0.54	3.0

[a] J_{sc} as calculated by integrating the EQE spectrum with the AM1.5 G spectrum.

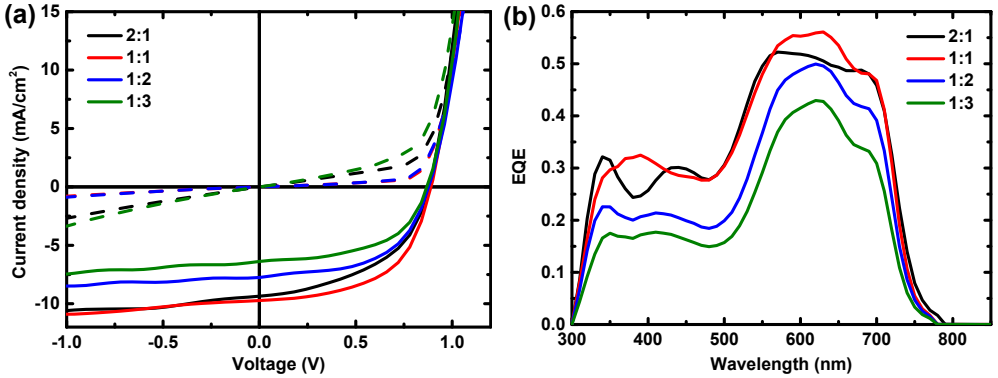

Fig. S6 (a) *J-V* characteristic under white light illumination and (b) EQE of the PCLDPP:PCBM solar cells fabricated from $CHCl_3$/DIO (0.5%) with different ratio of donor to acceptor.

Table S3. Characteristics of PCLDPP:PCBM (1:1) solar cells fabricated from $CHCl_3$/DIO (0.5%) with different thickness of active layers.

Thickness (nm)	J_{sc}[a] (mA/cm²)	V_{oc} (V)	FF	PCE[a] (%)
75	7.7	0.87	0.59	3.9
95	9.7	0.89	0.56	4.8
110	9.0	0.88	0.58	4.7
140	9.4	0.88	0.56	4.6

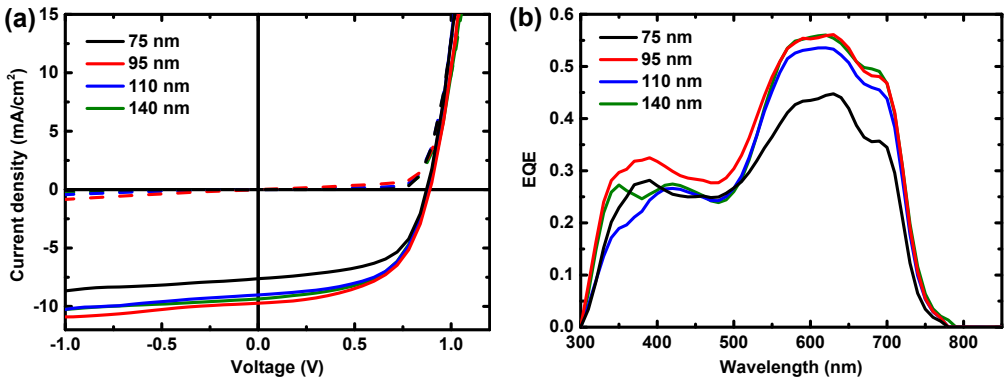

Fig. S7 (a) *J-V* characteristic under white light illumination and (b) EQE of the PCLDPP:PCBM (1:1) solar cells fabricated from $CHCl_3$/DIO (0.5%) with the different thickness.

6. Solar cells of PCLDPP:SdiPBI

Table S4. Characteristics of PCLDPP:SdiPBI (1:1) solar cells fabricated from chloroform with different content of DIO as additive.

Solvent	Thickness (nm)	J_{sc}[a] (mA/cm^2)	V_{oc} (V)	FF	PCE[a] (%)
$CHCl_3$/DIO (0.2%)	110	5.0	0.91	0.37	1.7
$CHCl_3$/DIO (0.5%)	100	5.2	0.94	0.35	1.7
$CHCl_3$/DIO (1%)	105	5.0	0.94	0.49	1.8

[a] J_{sc} as calculated by integrating the EQE spectrum with the AM1.5 G spectrum.

When using chloform without additive or increasing DIO content to 2.5%, the devices performed large leakage current with very low PCE.

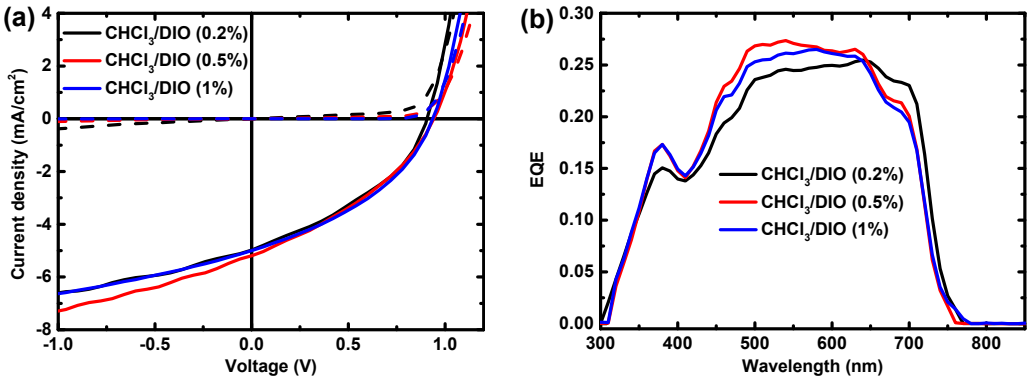

Fig. S8 (a) *J-V* characteristics under white light illumination and (b) EQE of the PCLDPP:SdiPBI (1:1) solar cells fabricated from $CHCl_3$ with different content of DIO as additive.

Table S5. Characteristics of PCLDPP:SdiPBI solar cells fabricated from $CHCl_3$/DIO (1%) with different ratio of donor to acceptor.

Ratio	Thickness (nm)	J_{sc}[a] (mA/cm^2)	V_{oc} (V)	FF	PCE[a] (%)
3:1	95	4.8	0.90	0.39	1.7
2:1	120	6.1	0.92	0.42	2.4
1:1	105	5.0	0.94	0.49	1.8
1:2	120	4.1	0.94	0.32	1.2

[a] J_{sc} as calculated by integrating the EQE spectrum with the AM1.5 G spectrum.

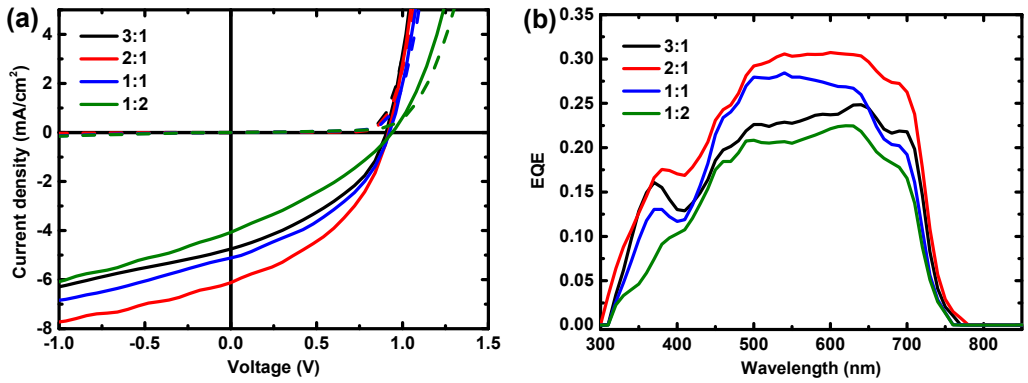

Fig. S9 (a) *J-V* characteristic under white light illumination and (b) EQE of the PCLDPP:SdiPBI solar cells fabricated from $CHCl_3$/DIO (1%) with different ratio of donor to acceptor.

Table S6. Characteristics of PCLDPP:SdiPBI (2:1) solar cells fabricated from $CHCl_3$/DIO (1%) with different thickness of active layers.

Thickness (nm)	J_{sc}[a] (mA/cm^2)	V_{oc} (V)	FF	PCE[a] (%)
70	4.0	0.91	0.43	1.6
90	4.9	0.91	0.40	1.8
120	6.1	0.92	0.42	2.4
160	5.4	0.91	0.37	1.8

[a] J_{sc} as calculated by integrating the EQE spectrum with the AM1.5 G spectrum.

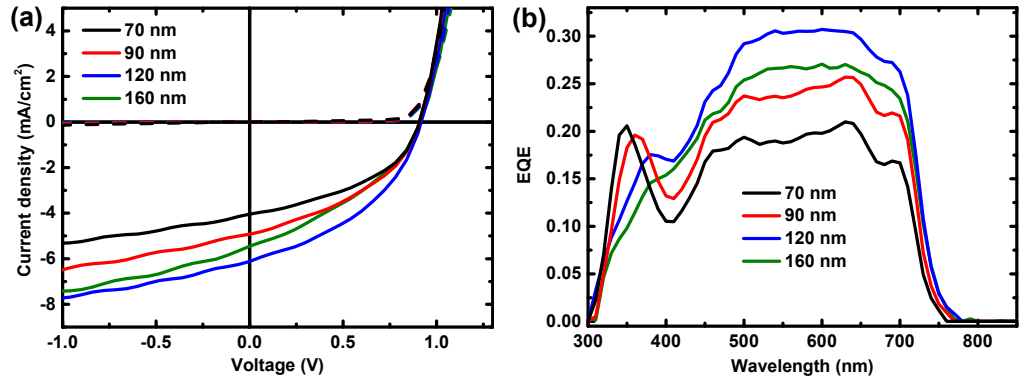

Fig. S10 (a) *J-V* characteristic under white light illumination and (b) EQE of the PCLDPP:SDiPBI (2:1) solar cells fabricated from $CHCl_3$/DIO (1%) with the different thickness.

7. Solar cells of PCLDPP:SdiPBI-S

Table S7. Characteristics of PCLDPP:SdiPBI-S (1:1) solar cells fabricated from chloroform with different content of DIO as additive.

Solvent	Thickness (nm)	J_{sc}[a] (mA/cm^2)	V_{oc} (V)	FF	PCE[a] (%)
$CHCl_3$/DIO (0.2%)	90	5.3	0.98	0.30	1.6
$CHCl_3$/DIO (0.5%)	120	7.6	0.98	0.42	3.1
$CHCl_3$/DIO (1%)	120	6.7	0.96	0.53	3.5

[a] J_{sc} as calculated by integrating the EQE spectrum with the AM1.5 G spectrum.

When using chloform without additive or increasing DIO content to 2.5%, the devices performed large leakage current with very low PCE.

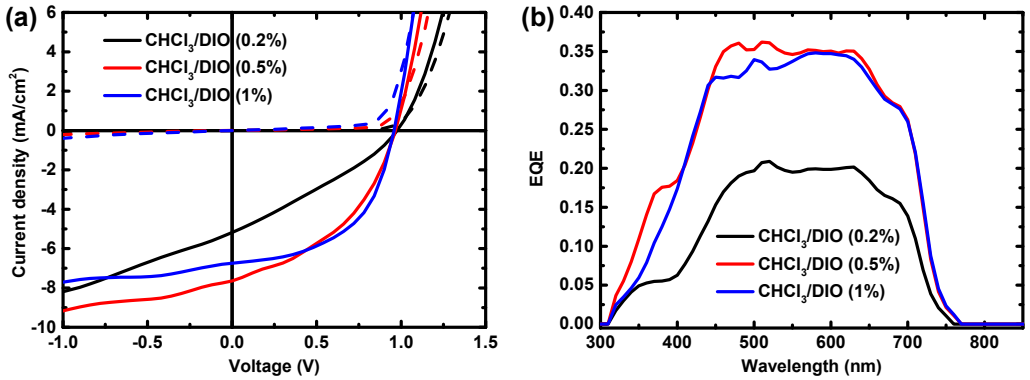

Fig. S11 (a) *J-V* characteristics under white light illumination and (b) EQE of the PCLDPP:SdiPBI-S (1:1) solar cells fabricated from $CHCl_3$ with different content of DIO as additive.

Table S8. Characteristics of PCLDPP:SdiPBI-S solar cells fabricated from $CHCl_3$/DIO (1%) with different ratio of donor to acceptor.

Ratio	Thickness (nm)	J_{sc}[a] (mA/cm^2)	V_{oc} (V)	FF	PCE[a] (%)
2:1	110	5.3	0.95	0.54	2.8
1:1	120	6.7	0.96	0.53	3.5
1:2	110	6.3	0.96	0.48	2.9

[a] J_{sc} as calculated by integrating the EQE spectrum with the AM1.5 G spectrum.

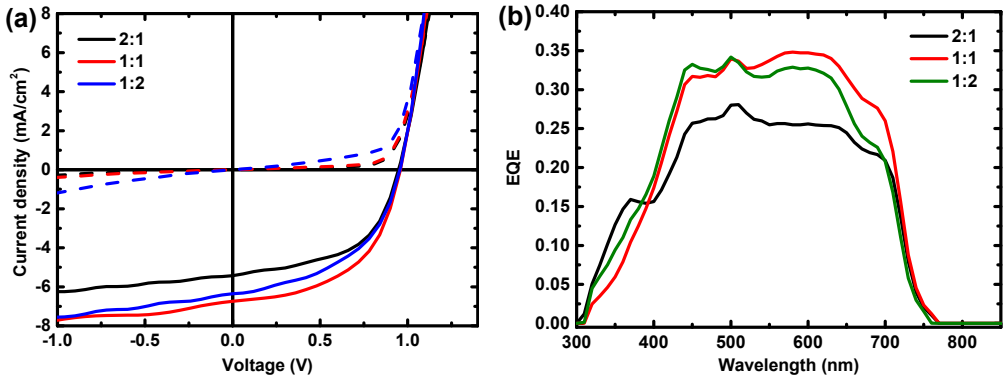

Fig. S12 (a) *J-V* characteristic under white light illumination and (b) EQE of the PCLDPP:SdiPBI-S solar cells fabricated from $CHCl_3$/DIO (1%) with different ratio of donor to acceptor.

Table S9. Characteristics of PCLDPP:SdiPBI-S (1:1) solar cells fabricated from $CHCl_3$/DIO (1%) with different thickness of active layers.

Thickness (nm)	J_{sc}[a] (mA/cm²)	V_{oc} (V)	FF	PCE[a] (%)
90	6.1	0.96	0.45	3.2
100	6.6	0.95	0.53	3.3
120	6.7	0.96	0.53	3.5
160	6.7	0.94	0.49	3.1

[a] J_{sc} as calculated by integrating the EQE spectrum with the AM1.5 G spectrum.

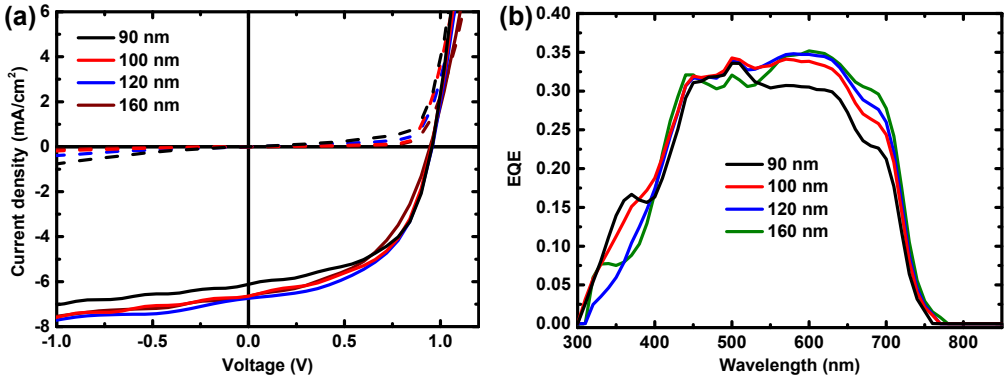

Fig. S13 (a) *J-V* characteristic under white light illumination and (b) EQE of the PCLDPP:SdiPBI-S (1:1) solar cells fabricated from $CHCl_3$/DIO (1%) with the different thickness.

8. FETs based on pure and blended thin films.

Table S10. Field effect hole mobilities of PCLDPP and blended thin films in a BGBC configuration.

	Annealing temp	μ_h [$cm^2\ V^{-1}\ s^{-1}$]	V_T [V]	I_{on}/I_{off}
PCLDPP	80 °C	2.6×10^{-2}	-8.8	2.7×10^{8}
PCLDPP:PCBM	130 °C	1.0×10^{-1}	-15.1	8.2×10^{4}
PCLDPP:SdiPBI	130 °C	4.9×10^{-2}	-31.3	3.6×10^{4}
PCLDPP:SdiPBI-S	80 °C	2.0×10^{-2}	-23.6	1.8×10^{3}

9. Photoluminescene spectra of pure molecular thin films

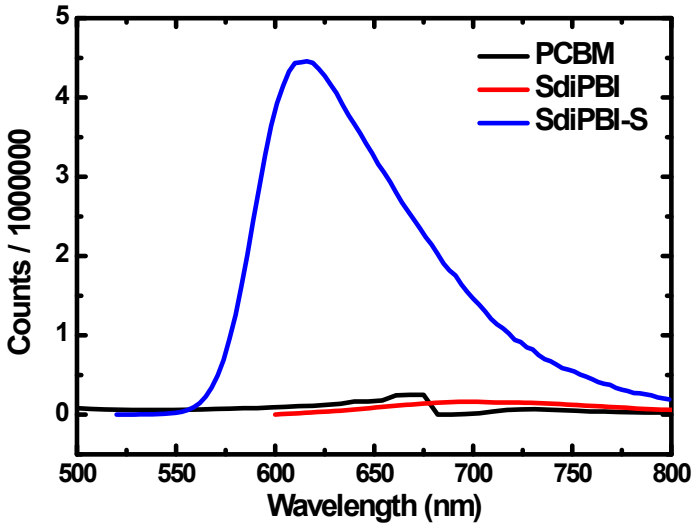

Fig. S14 Photoluminescence spectra of the electron acceptor thin films. The excitation wavelength is 400 nm, 530 nm and 504 nm for PCBM, SdiPBI and SdiPBI-S.

10. 2D-GIWAXS patterns of PCLDPP, SdiPBI and SdiPBI-S thin films

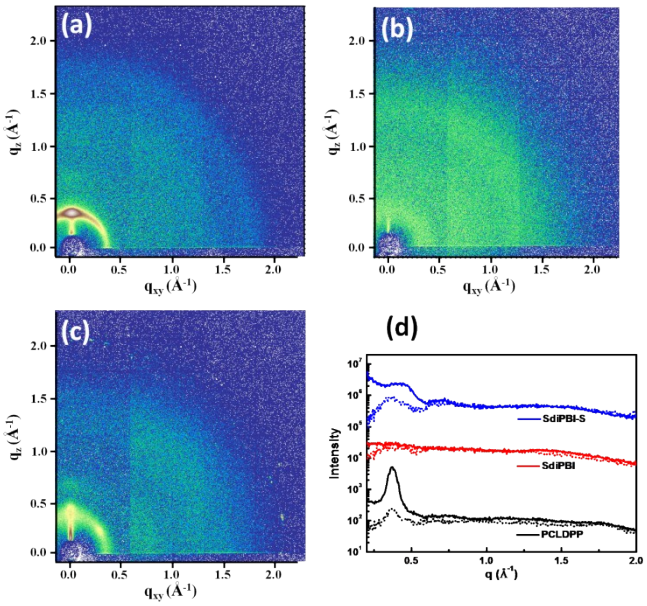

Fig. S15 Characteristics of the (a) PCLDPP, (b) SdiPBI and (c) SdiPBI-S fabricated from $CHCl_3$. (a) – (c) 2D-GIWAXS patterns, and (d) the out-of plane (solid lines) and in-plane (dash lines) of the corresponding 2D-GIWAXS patterns.